Lattice models of failure: Sensitivity to the local dynamics

Andrei Gabrielov*
International Institute of Earthquake Prediction Theory and Mathematical Geophysics, Russian Academy of Sciences, Moscow, Russia;
Department of Geology, Cornell University, Ithaca, New York 14853;
Institute of Geophysics and Planetary Physics, University of California, Los Angeles, California 90024

William I. Newman
Departments of Earth and Space Sciences, Astronomy, and Mathematics, University of California, Los Angeles, California 90024

Leon Knopoff
Institute of Geophysics and Planetary Physics and Department of Physics, University of California, Los Angeles, California 90024
(Received 8 March 1994)

Quasistatic lattice models to explore scaling and other properties of failure events, including earthquakes, are characterized by the presence of two or more time scales. We show that there is a remarkable degree of variability in the qualitative behavior of these models: In one model with periodic boundary conditions, which simulates a moving dislocation or avalanche model of fracture, the trajectories are always periodic in both one and two dimensions. In another quasistatic model which simulates a growing coherent crack, the trajectories are either periodic or chaotic, depending on the initial conditions. Characteristic behaviors derived from analytic results are illustrated by numerical simulations.

PACS number(s): 05.45.+b, 46.30.Nz, 64.60.Ak, 91.60.Ba

I. INTRODUCTION

In the model of self-organized criticality due to Bak *et al.* [1], a homogeneous lattice system organizes itself into a critical state via fluctuations regulated by the local rules for the dynamics. If the local rules obey a conservation law, the system will develop a scale-independent distribution of sizes of events that is valid on all scales. Bak and Tang [2] proposed that this model had application to the simulation of earthquake faulting. Kadanoff *et al.* [3] showed that the size distributions are sensitive to the local dynamics and may belong to different universality classes. In the model [1], dissipation is only possible at the edge of the lattice, implying the existence of a massive inhomogeneity at the edge of an otherwise homogeneous system. In models with nonconservative local dynamics, dissipation can take place in the interior of the lattice, and a number of models with dissipative dynamics have been explored [4–7]. These dissipative models are similar to a dynamical lattice model of earthquake occurrence introduced by Burridge and Knopoff [8] and explored in depth by Carlson and Langer [9,10] and Carlson [11]. Matsuzaki and Takayasu [12] and Lomnitz-Adler *et al.* [13] have explored the ability of a dissipative lattice system without inertia but with nonlocal dynamics, to organize itself into a critical state. The latter authors also found that the presence or absence of a critical state depends delicately on the choice of the rules, and is very sensitive to small changes. Other models explore systems that involve nonlocal dynamics, other fracture geometries, etc. [14–16].

In this paper, we consider lattice models similar to the above with dissipation but without inertia, i.e., the system is massless. We are concerned with failure or avalanche models, in general, and earthquake models, in particular. Readers are advised to consider terms such as earthquake events and fracture as metaphors for a broad range of phenomena including but not confined to seismicity and material failure. Let "slow" or tectonic time be the interval between fracture events, during which the loading increases the level of stress in the solid. This stress is then released through a sequence of one or more breaks in "fast" time, which is the time needed for fractures to develop. In the case of real earthquakes, these two time scales differ by seven orders of magnitude or more—the slow time scale can be the order of a century, while the fast time scale may be as long as one or two minutes for the largest earthquakes.

We study a class of deterministic models where both time and stress are *continuous* variables and where the loading proceeds at a uniform rate at all lattice sites. This was first done by Burridge and Knopoff [8] and later by others [5–7,17]. This class of models, as with those considered in [9–11,15] is (stress) dissipative, in contrast with the stress conservative model of [1]. Olami *et al.* [7] have shown that this class of lattice models is formally

*Now with the Department of Mathematics, University of Toronto, Toronto, Ontario, Canada M5R 2P7.

equivalent to the zero-mass limit of the Burridge-Knopoff spring-block model with different friction laws. For a scalar particle model with uniform spacing, the value of the total force and the stress on a lattice site are equivalent. For convenience we use the term stress for this quantity.

We employ a lattice model whose elements slowly accumulate stress up to a certain threshold of strength; the accumulated stress is then rapidly released in fast time. Part of the released stress is redistributed between other elements and part is dissipated locally. We construct a sequence of the slow times and intensities of the fracture events. In all of our experiments we consider uniform lattices with periodic boundary conditions.

We consider two variants of the model, which we call *series* and *parallel* models, both having identical structure and laws of failure; the only difference between the models is the order of stress release and redistribution in fast time.

In the series model, the stress is fully released immediately when the stress on an element achieves the threshold of strength. Then part of the released stress is added to the neighboring elements. The same procedure is now applied to all neighbors that have stress greater than or equal to the threshold. The process is repeated until no elements have stresses exceeding the threshold. In this case, the stress release rate is presumed to be faster than the stress redistribution rate.

In the parallel model, an element breaks when the stress arrives at the threshold of strength, and starts to release its stress in fast time. In this case, part of the released stress is *simultaneously* added to the neighboring elements as the stress on the first element drops. This process continues until all the stress on the broken element is released or until the stress on some of its neighbors arrives at the threshold. In the latter case, the neighboring element breaks and begins to release and redistribute its stress in the same manner, until finally no more elements break. This corresponds to the case when the stress release rate is slower than the stress redistribution rate.

We show that these two models lead to markedly different dynamical histories. For a uniform lattice with periodic boundary conditions, we find and can prove analytically that for most initial conditions the parallel model produces essentially chaotic behavior while the series model always converges to a complex but periodic trajectory.

II. MODELS

In these quasistatic models, the process of readjustment of the accumulated stress at a site involves two physically different time scales, which are the time needed for the bond at that site to fail, or the stress release time, and the time needed for the released stress to be transferred to the neighboring sites, or the stress transfer time. For simplicity and without loss of generality, we set the stress accumulation rate and the stress threshold, i.e., the strength of the elements, numerically equal to unity.

Both the stress release and stress transmission time scales are much smaller than the loading or tectonic time scale. The ratio of these two fast times is a parameter describing a broad class of models of failure with two limiting cases of particular interest.

A. Series model

In the first case, which is similar to most other quasistatic lattice models [1,4–7], the stress transmission time is much longer than the stress release time. In an extended lattice, this may correspond to the quasistatic model for a moving dislocation or to the avalanche analogue of a fracture. In this case, we observe a "series" of stress release events, followed by a series of transmission events followed by a series of release events, and so on. Dissipation is introduced through a dissipation parameter S which is the fraction of the accumulated stress that is lost to the system; the remaining fraction $1 - S$ is redistributed equally among the nearest neighbors.

Since a site that receives transferred stress from a neighboring ruptured site can achieve a stress level greater than its threshold, there are at least two variants of the series model. In case a, the stress level at a fracturing site is reduced by a fixed amount, while in case b, the stress level at the new site is reduced to zero. Let σ_{ij} be the stress level at a given site (i, j). In case a,

$$\sigma_{ij} \to \sigma_{ij} - 1 \text{ and } \sigma_{nn} \to \sigma_{nn} + p \quad , \tag{2.1}$$

if $\sigma_{ij} \geq 1$, where the interaction parameter $p \equiv (1-S)/2d$ and d is the dimensionality of the lattice. This model is similar to the models explored by Refs. [1,5] and [18]; we present some new results for this model. In case b,

$$\sigma_{ij} \to 0 \text{ and } \sigma_{nn} \to \sigma_{nn} + p\sigma_{ij} \tag{2.2}$$

if $\sigma_{ij} \geq 1$. This model can also be related to [6,7,19], and again we present new results for this model.

In case a, it can be shown that the sequence of events in slow time is *independent* of the order of breaks in fast time. In this respect, the model is similar to the abelian sandpiles introduced in [20]. As a result of this commutative property, it is not necessary for the stress level of newly released sites to be adjusted synchronously, as long as the stress drop experienced by each of these sites is the same. In case b, it is essential that stresses be reduced at failed sites in proper sequence; otherwise, the behavior obtained is quantitatively, but evidently not qualitatively, dependent upon the order of the stress drop. In the numerical and analytic results below we discuss these variants of the series model.

B. Parallel model

In the second case, the stress release time is much longer than the transmission time. As a given element releases its accumulated stress, its nearest neighbors immediately receive a proportionate increase in their stress.

The stress release and redistribution take place in "parallel" among the appropriate elements. In this model, a neighboring site can reach the threshold of rupture while the site which initiated the release is still in the process of releasing stress. In an extended lattice, this may correspond to a quasistatic model for a growing crack, with motions correlated along its extent, and not dissimilar from the models of [12,13]. In this redistribution model, we cannot distinguish between cases a and b as in the series model, because failure always occurs at precisely the stress threshold, which is reached gradually within fast time. Again we define the failure threshold by $\sigma_{ij} = 1$. When an element fails, the elements respond in fast time τ according to the relations

$$\frac{d\sigma_{ij}}{d\tau} \to \frac{d\sigma_{ij}}{d\tau} - 1 \text{ and } \frac{d\sigma_{nn}}{d\tau} \to \frac{d\sigma_{nn}}{d\tau} + p \quad . \tag{2.3}$$

These relations hold until $\sigma_{ij} = 0$ whereupon

$$\frac{d\sigma_{ij}}{d\tau} \to \frac{d\sigma_{ij}}{d\tau} + 1 \text{ and } \frac{d\sigma_{nn}}{d\tau} \to \frac{d\sigma_{nn}}{d\tau} - p \quad . \tag{2.4}$$

When $d\sigma_{ij}/d\tau = 0$ for all sites, we return to the slow time scale.

III. EXAMPLE: THREE-ELEMENT CONFIGURATION

We begin by looking at a configuration of three elements connected in a closed chain, which has both a series and a parallel realization, before proceeding to the case of large lattices. When any element fails, a fraction p of its released stress is transferred to each of the other two elements, and a fraction $S = 1 - 2p$ is dissipated. The simple three dimensional phase space of this reduced system permits detailed analytic investigation.

This model can be described by a Poincaré surface of section, defined without loss of generality, by plotting the stress level σ_2 and σ_3 of each of the surviving elements 2 and 3 when element 1 fails. In Fig. 1, we show the geometry of the Poincaré surface of section for series case a. The regions with indicial notations correspond to various periodic trajectories. The indicial notation "1, 2, 3" describes periodic trajectories in which each element fails separately in the order given; we refer to this sequence of *isolated* failures as "single breaks." On the other hand, "1-2, 3" refers to a situation where the failure of element 1 causes element 2 to fail instantly, and then after some time element 3 fails. Finally, "1-2-3" refers to a situation in which all three elements fail simultaneously. One can readily show that all of these trajectories are periodic. The hatched region is not periodic, but subsequent breaks will bring any point from the hatched region into one of the periodic trajectory domains.

In case b, only the shaded regions "1, 2, 3" and "1, 3, 2" (i.e., single breaks) are periodic and we can show that *all* other regions of the σ_2-σ_3 plane arrive, after a finite number of breaks, in one of these two periodic domains.

In the parallel case, the single break situations "1, 2, 3" or the inverse, remain periodic while the behavior in the other cases is more complicated. It can be shown that

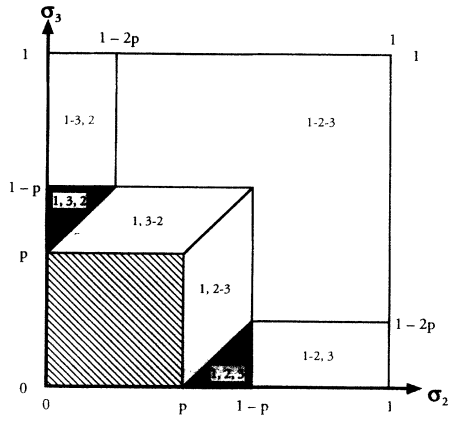

FIG. 1. The Poincaré section $\sigma_1 = 1$ for the three-element configuration, series redistribution model for both cases a and b. Areas designated by indices correspond to different types of periodic trajectories. Every trajectory starting in the hatched area is unstable and moves into one of the periodic areas. In case b, only areas with single breaks, i.e., those designated by $1, 2, 3$ and $1, 3, 2$, (shaded in the figure) are stable.

the mapping is area preserving and hence the complexity which it manifests has the signature of Hamiltonian chaos. The map for the case $p = 2/5$ ($S = 1/5$) is shown in Fig. 2. We exploit the fact that Fig. 2 is symmetric about a diagonal. Below the diagonal, the black area identifies a chaotic region. We represent here one chaotic trajectory; it is everywhere dense, but does not have pos-

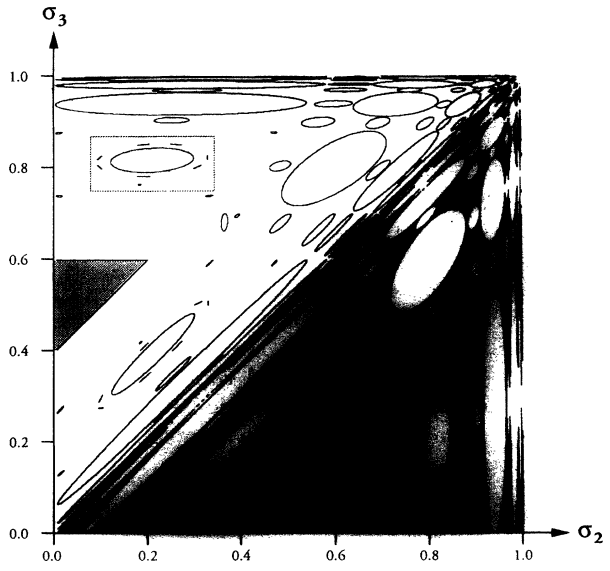

FIG. 2. Poincaré section $\sigma_1 = 1$ for the three-element configuration, parallel redistribution model, $p = 2/5$ or $S = 1/5$. The white triangles correspond to periodic trajectories with single breaks (as in Fig. 1), while the white ellipses correspond to families of invariant tori with quasiperiodic behavior. The figure is symmetric about the diagonal, but the above- and below-diagonal portions highlight different features of the problem. Below the diagonal, the black area defines the chaotic region, while above the diagonal, the boundary between the chaotic and regular behavior is displayed.

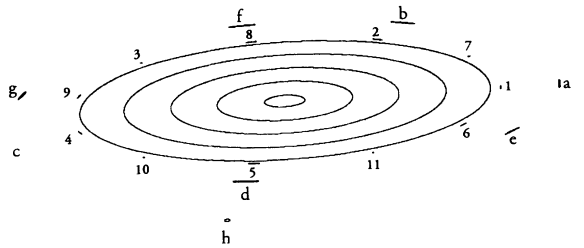

FIG. 3. Expansion of the boxed region of Fig. 2. One of the families of invariant tori, with two satellite families consisting of 11 and eight elements, are shown. The numbers $1-11$ and letters $a-h$ specify the ordering of quasiperiodic trajectories in the two satellite families.

itive measure because it is a countable set. Indeed, a continuum of chaotic trajectories coexist in the same region. Above the diagonal, we describe the boundaries between the regions of chaotic and regular behavior. The triangular areas of periodic behavior (shaded) shown in Fig. 1 also appear in Fig. 2. There is as well an infinite number of elliptical areas, each of which is filled by a family of invariant tori with quasiperiodic behavior. In Fig. 3, we show in detail one of these regular regions, which is identified by a box in the upper left of Fig. 2. This is an area having a continuum of tori together with "satellites" which are themselves families of invariant tori. In the figure, we identify one group of 11 satellites designated by the numbers 1–11, and another of eight satellites designated by the letters a–h. Any orbit which originates in one of these satellites progresses to another satellite in the same group in the order shown in the figure.

Unlike many dynamical systems encountered in physics for which empirical evidence of chaotic behavior has been advanced, we are able to show *rigorously* the presence of chaos in the parallel case. We exploit the inherent symmetry of this system as follows. A trajectory may take us from one face of the unit cube, say with $\sigma_1 = 1$ to another with $\sigma_2 = 1$ or $\sigma_3 = 1$. Suppose the trajectory goes from $\sigma_1 = 1$ to $\sigma_2 = 1$; then, we map $\sigma_3 \to \sigma_2$, $\sigma_1 \to \sigma_3$ cyclically, and so on. The symmetry of this system guarantees that this map, which we denote by P, is well defined, i.e., is one to one, and is area preserving although it is not continuous.

To prove that the behavior of the three-element parallel configuration is chaotic, consider the polygon (see Fig. 4) with vertices

$$A = \left(\frac{7}{20}, \frac{3}{4}\right), \; B = \left(\frac{1}{5}, \frac{3}{5}\right), \; C = \left(0, \frac{3}{5}\right),$$
$$D = \left(0, \frac{66}{95}\right), \; E = \left(\frac{16}{35}, \frac{6}{7}\right), \tag{3.1}$$

lying in the area between the shaded triangle and the boxed domain in Fig. 2. The line AC separates this polygon into a triangle ABC and a quadrangle $ACDE$. It can be shown that $Q \equiv P \circ P$ (i.e., the map P taken twice) is linear on ABC and on $ACDE$, that is,

$$Q(\sigma_2, \sigma_3) = \left(\sigma_2 - \frac{7}{3}\sigma_3 + \frac{7}{5}, \sigma_3\right) \quad \text{in } ABC \quad , \tag{3.2}$$

and

$$Q(\sigma_2, \sigma_3) = \left(\frac{4}{3}\sigma_2 - \frac{19}{9}\sigma_3 + \frac{22}{15}, -\sigma_2 + \frac{7}{3}\sigma_3 - \frac{4}{5}\right) \tag{3.3}$$

in ACDE.

Images of ABC and $ACDE$ intersect both ABC and $ACDE$ producing a "horseshoe [21]." As a result of Smale's Theorem [21], a subset in the unit square, invariant under Q and Q^{-1}, has the characteristic structure of a Cantor set.

The point $X = \left(\frac{4}{25}, \frac{18}{25}\right)$ in $ACDE$ is a fixed point of Q with eigenvectors $(3 \mp \sqrt{85}, 6)$ and eigenvalues $(11 \pm \sqrt{85})/6$, which define the stable and unstable separatrices of Q. A segment $XY \subset ACDE$ of the unstable separatrix of Q extends to XY_2 under Q. Let YZ be the intersection of XY_2 with ABC. Then, the image Y_1Z_1 of YZ under Q intersects transversely the segment VX of a stable separatrix of Q, producing a "homoclinic" structure [21], which satisfies the formal criterion for (homoclinic) chaos. Images of the unstable separatrix under eight iterations of Q are shown in Fig. 4.

From this formal demonstration of the chaotic character of the three-element configuration, we turn our attention to the numerical results for the series and parallel lattice models.

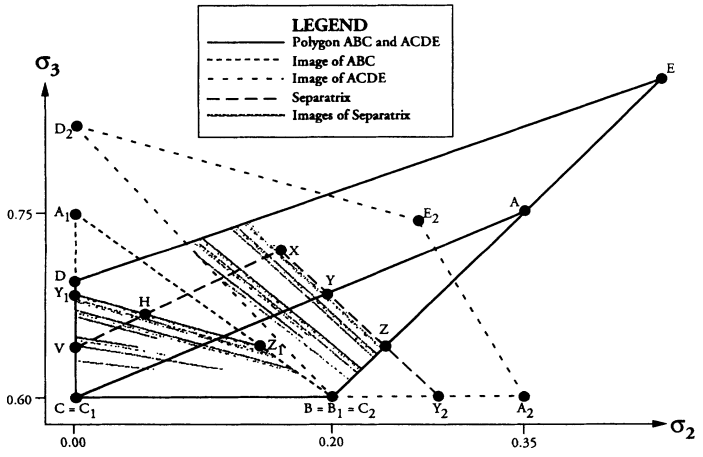

FIG. 4. Homoclinic chaos in the three-element configuration, parallel redistribution model for $p = 2/5$ ($S = 1/5$). X is a fixed point of the Poincaré map, while H is a homoclinic point, i.e., it is the intersection of the stable and unstable separatrices of the Poincaré map at X.

IV. RESULTS: PERIODIC LATTICE

Consider a periodic lattice of arbitrary dimensionality d and interaction parameter p, under conditions of case a of the series redistribution model with fixed stress drop. Let the system, starting in slow time from a state $\sigma_i(t)$, undergo an arbitrary sequence of consecutive breaks that includes all the elements in the system, each of them only once, during a time period S. Then one can show that $\sigma_i(t+S) = \sigma_i(t)$ for all i where t denotes the time and the state $\sigma_i(t)$ belongs to a periodic trajectory with period S.

Such a trajectory, where each element fails only once in a period, will be referred to as a *normal trajectory*. For any initial state (see Appendix A), the system arrives at a normal trajectory after a finite number of breaks.

The period of the trajectory is S because the units of stress and time are chosen so that the stress drop is equal to S and the rate of stress loading is unity. In an equivalent block model formulation [7], the value S corresponds to the rigidity of the loading spring. If we choose the units to make the stress drop and the velocity of loading constant, then the period scales as $1/S$.

What is notable is that the periodic part of the trajectory appears to be "chaotic" within a single period. We refer to this phenomenon as "periodic chaos." In Fig. 5, we show the distribution of break sizes as a function of time during one period for a 300×300 lattice with $S = 0.01$ for two randomly chosen initial stress distributions. Both time histories appear to be "chaotic" but are manifestly different from each other. There is no hint in this figure that the trajectory could be periodic. Indeed, this result poses a warning that abbreviated investigations of these phenomena can lead to grossly incorrect conclusions about the nature of the phenomena.

Size-frequency diagrams generated from one periodic trajectory appear to be crudely power law in character and display a characteristic logarithmic slope near -1 in the central part of the distribution when S is sufficiently small. This is illustrated in Fig. 6 for the two periodic trajectories shown in Fig. 5. The two distributions are remarkably similar, despite having been produced by two randomly chosen periodic trajectories.

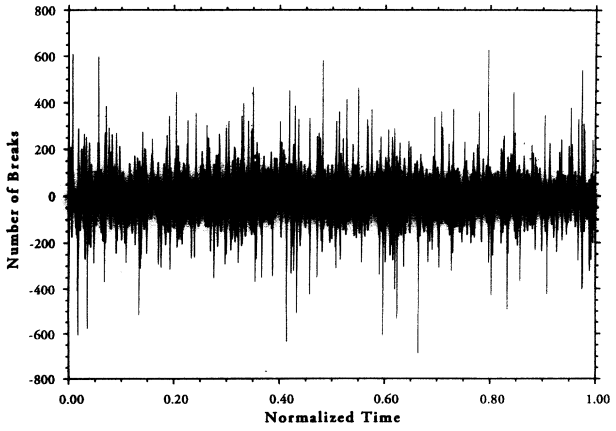

FIG. 5. Two typical realizations of break size as a function of time for one period of a periodic trajectory in the series redistribution model case a, 300×300 lattice and $S = 0.01$ displaying periodic chaos. The results shown are for two randomly selected periodic trajectories of the same model: the two sets of results are displayed above and below the time axis, respectively.

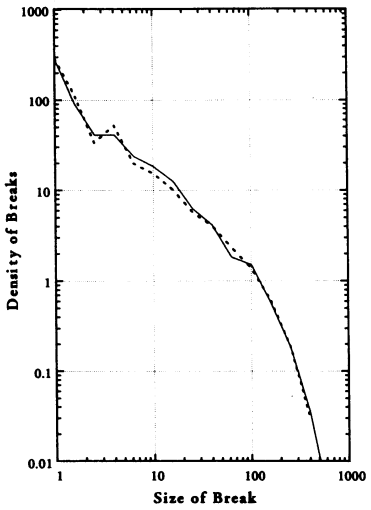

FIG. 6. The size-frequency distribution for two periodic trajectories periodic chaos in the series redistribution model case a; 300×300 lattice with $S = 0.01$. Size is defined to be the number of elements that break in a single cascade event.

For a one-dimensional lattice, the structure of the phase space in case a, i.e., with fixed stress drop, of the series redistribution model can be investigated analytically (see Appendix B). Consider a one-dimensional lattice of size N subdivided into n (connected) clusters of different sizes. The volume of all normal trajectories with n clusters is equal to

$$V(n,N) = \frac{N}{n}\binom{N+n-1}{2n-1} S^n p^{N-n} \quad . \tag{4.1}$$

Let $V(N) = \sum_{n=1}^{N} V(n,N)$ be the total volume of all periodic trajectories. Then

$$V(N) \propto \left(\frac{1+\sqrt{1-4p^2}}{2}\right)^N \quad \text{as } N \to \infty \quad . \tag{4.2}$$

An estimate of the mean value $A_j(N)$ of the number of clusters of size j for a randomly chosen periodic trajectory is the analytic size-frequency distribution:

$$A_j(N) = \frac{jN}{V(N)} \sum_{n=1}^{N} \binom{N+n-j-2}{2n-3} S^n p^{N-n} \quad , \tag{4.3}$$

so that

$$A_j(N) \propto jNS\sqrt{\frac{1-2p}{1+2p}} \left(\frac{2p}{1+\sqrt{1-4p^2}}\right)^{j-1} \tag{4.4}$$

for $N \gg j$. This analytic result is substantially different from the size-frequency distribution obtained numerically in the two-dimensional case, a feature also noted by Bak

et al. [1]. As $S \to 0$, the large events dominate the distribution, while small events scale in proportion to size (a feature also noted by Bak *et al.* [1]). These results demonstrate a fundamental difference between one- and two-dimensional models.

In case *b* of the series model, as well as in the case of parallel redistribution, periodic behavior appears for a much smaller set of states, in which only single breaks are allowed. (It is easy to show that both of the series cases and the parallel case are equivalent on the set of single breaks [22].) If N is the number of elements in the lattice, then the part of the phase space occupied by normal trajectories with single breaks has volume S^N and consists of $N!$ identical simplexes, a result that has been confirmed analytically (see Appendix C).

Computer simulations show that, in the case of series redistribution with a fixed healing threshold, the set of these simplexes is a global attractor, and a trajectory with *any* initial state becomes periodic after a finite, but generally very large number of breaks. In the short term, the trajectory becomes "almost" periodic, with multiple-breaks occurring with a "period" shorter than S. With the passage of time, each multiple break decomposes into a sequence of single breaks; however, the sequence of single breaks preserves the memory of its multiple-break origin and remains localized in space and time, as shown in Fig. 7 for a one-dimensional system of 200 elements with $S = 0.1$. Figure 8 shows two time intervals extracted from the sequence shown in Fig. 7 to illustrate the transition of multiple-break behavior into single-break behavior.

In the parallel redistribution model, the behavior outside of these simplexes is, in general, seemingly chaotic. We considered situations where the initial values of the stress are taken to be uniformly distributed between 0 and 1. In Fig. 9, we show a time stress plot for a 20×20 lattice with $S = 0.1$. There is a natural time scale which coincides with S in the "stress-accumulation-release cycle." On the other hand, intermittency on a time scale that is long compared with S is evident. This may be observed in two noncontiguous segments of this time series,

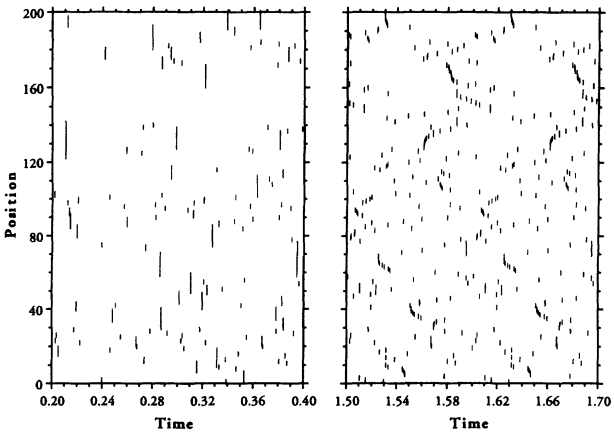

FIG. 8. Two time intervals selected from Fig. 7 to illustrate the transition from multiple- to single-break behavior.

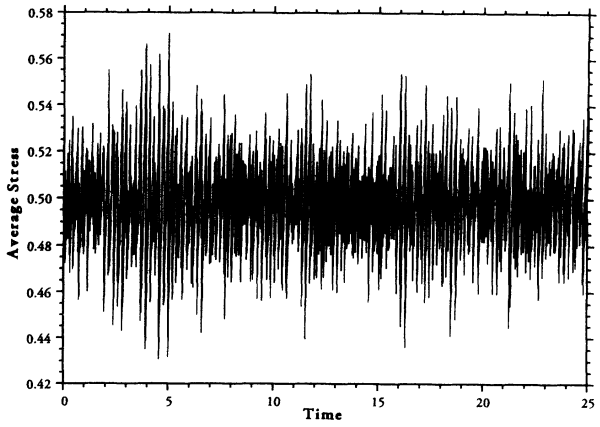

FIG. 9. Intermittency in the parallel model, on a 20×20 lattice for $S = 0.1$.

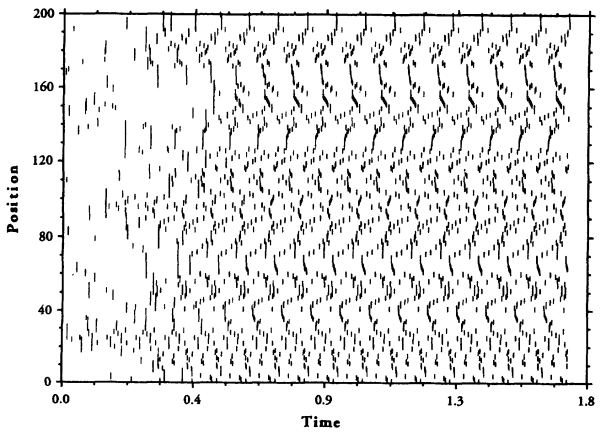

FIG. 7. The space-time distribution for a periodic trajectory in the series model, case *b*, displaying significant localization. For sufficiently long times, all events are single breaks.

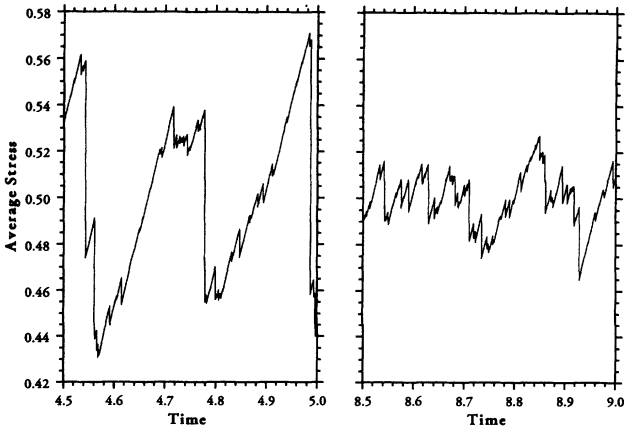

FIG. 10. Two noncontiguous time segments from the previous plot, revealing the nonstationary character of the intermittency.

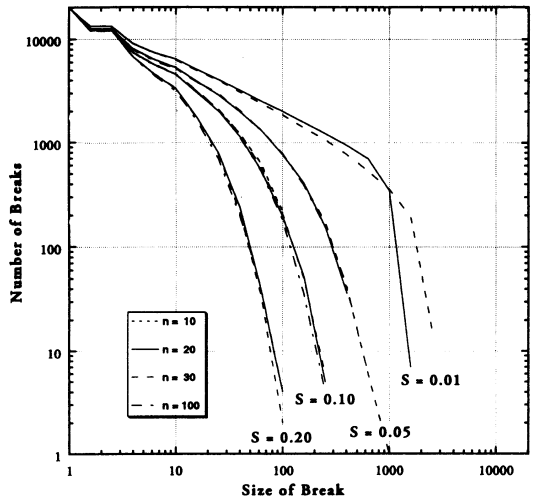

FIG. 11. The cumulative size-frequency distribution for the parallel case for different sizes of the two-dimensional lattice, and for different values of S. As the lattice size n increases, the distributions seem to converge to the Γ distribution.

which we display in Fig. 10. Finally, we have computed cumulative size-frequency distributions for this case for different values of the dissipation parameter S and lattice size n (Fig. 11); the distributions are independent of n for a given value of S. The distribution appears to be consistent with a power law with an exponential cutoff which depends upon the value of S; this distribution is called the gamma distribution in the statistical literature. However, for small values of S, the exponential cutoff migrates to infinity and, in the apparent power-law regime of the distribution, the power-law index lies between -1 and -2, a result that is quite different from the situation encountered in the series model.

V. CONCLUSIONS

Quasistatic lattice models of failure with dissipation have been employed recently by a number of authors to explore the scaling and other properties of catastrophic events including earthquakes. These models are representative samples of a broad spectrum of physical situations described by the presence of two or more characteristic time scales: a "slow" time with the interval between failure events associated with tectonic loading and a "fast" time associated with the fracture event itself. There are two broad classes of models characterized by their fast time dynamics: (i) the series model characterized by an instantaneous release of stress at a failed lattice site followed by the transfer of some fraction of that stress to neighboring lattice sites; and (ii) the parallel model characterized by a *relatively* slow release of stress at a failed site and an instantaneous transfer of some fraction of that stress to neighboring lattice sites. We have considered two versions of the series model; in case a the stress level at the failed lattice site is reduced to zero, and in case b the stress level is reduced by a fixed amount. These models yielded remarkably different qualitative behavior.

In the series model of a uniform periodic lattice containing N elements, part of the phase space consists of *periodic* trajectories. This part of the phase space is of positive measure, i.e., it occupies a finite part of the entire phase space. This set of periodic trajectories is a *global* attractor of the system: *any* initial state arrives at a periodic trajectory in finite time. In case a, these periodic trajectories may contain multiple breaks, in which many elements fail at the same time. For N large, the behavior during one period may appear to be chaotic, and displays an approximate "size-frequency" law $1/f$ as the dissipation parameter S goes to zero. We refer to this remarkable situation as "periodic chaos." In case b, the set of periodic trajectories is much smaller than in a, occupying a fraction S^N of the phase space. The rate of convergence to the periodic trajectory is much smaller In case b than in case a. The trajectory quickly enters an intermediate phase of behavior which includes multiple breaks that gradually decompose into a series of single breaks which are localized in space and in time.

In the parallel model, the set of periodic trajectories is also composed solely of single breaks. (We note that once a periodic trajectory composed of single breaks is achieved, the parallel model and both cases of the series model are equivalent.) In the phase space outside the periodic regime, most trajectories are chaotic producing a size-frequency relation which converges to a power law as the dissipation parameter S approaches zero, but the power-law differs from the former $1/f$ situation. Moreover, at time scales that are large compared with S, there is substantial intermittent behavior.

Finally, the three-element model is particularly remarkable in that it provides such complexity. Analytically, we have shown it to exhibit Hamiltonian chaos including homoclinic points and the presence of Smale horseshoes. In addition, we have derived an analytic size-frequency distribution from combinatoric considerations, which is markedly different from the two-dimensional case (cf. [1]).

ACKNOWLEDGMENTS

This work was initiated when A.G. visited UCLA and W.I.N. visited the Institute of Physics of the Earth, Moscow, under Environmental Protection Agreement 02.09-13 between the United States and the Union of Soviet Socialist Republics (host institutions: USGS and UCLA, and the USSR Academy of Sciences). Part of this work was performed on a visit of A.G. to UCLA under support of the Institute of Geophysics and Planetary Physics, UCLA, and on a visit of A.G. to Cornell University, under NSF Grant No. EAR-91-04624. We thank A. Zelevinsky for suggestions relevant to the combinatoric calculations. This research has been supported in part by the Southern California Earthquake Center, Pub. No. 4170, Institute of Geophysics and Planetary Physics, University of California, Los Angeles.

APPENDIX A: NORMAL TRAJECTORIES

Let us consider a periodic lattice of arbitrary dimensionality d, with an interaction parameter p and a dissipation parameter $S = 1 - 2dp > 0$. For any two sites i and j of the lattice, we define $p_{i,j} = p$ if i and j are nearest neighbors, $p_{i,j} = 0$ otherwise.

Proposition 1. In case a of the series redistribution model, let the system, starting in slow time from a state $\sigma = \{\sigma_i(t)\}$, undergo an arbitrary sequence of consecutive breaks that includes all of the elements in the system, each of them only once, during a time period S. Then $\sigma_i(t+S) = \sigma_i(t)$, for all i, and the state σ belongs to a periodic trajectory with period S. For arbitrary initial state, the system arrives at one of these periodic trajectories after a finite number of breaks.

Proof. After all of the elements break, at the moment in time $t+S$, the stress of the ith element becomes $\sigma_i(t+S) = \sigma_i(t)$ due to the loading in slow time S, wherein the stress increases by $2dp$ from the $2d$ broken neighbors, and decreases by 1 due to the stress drop.

Suppose now that the initial state σ does not satisfy the condition of Proposition 1. The same arguments as before show that no element can break twice during the time period S. Thus, if $N-K$ elements break during this period, $K > 0$, then the total stress of the system during the time period S increases by KS. Then, during each time interval S, the system would experience a net stress increase. As the total stress of the system cannot exceed N, we obtain a contradiction. Therefore, we must come to a periodic trajectory after a finite number of breaks.

APPENDIX B: PHASE SPACE STRUCTURE

We describe here the structure of the set of all periodic trajectories in case a of the series redistribution model for a uniform 1D periodic lattice of size N.

Consider an arbitrary subdivision of $(1,\dots,N)$ into n clusters of different sizes, and let $n_i \geq 0$ be the number of clusters of size i, so $n_1 + \cdots + n_N = n$, $n_1 + 2n_2 + \cdots + Nn_N = N$.

Proposition 2. The volume of all states generating periodic trajectories with sequence of n breaks containing n_i events of size i is equal to

$$V_{n_1,\dots,n_N} = N(n-1)!\prod_{i=1}^{N}\frac{i^{n_i}}{n_i!} \times S^n p^{N-n} \quad . \tag{B1}$$

Proof. Let us identify an initial state defined in Proposition 1 with an ordered sequence of n nonoverlaping connected clusters (i.e., fast time episodes) covering the lattice, containing n_i clusters of size i, and one distinguished (i.e., special) element in each cluster, namely, the first broken element. Simple combinatorial considerations show that the number of these objects is equal to

$$Nn!(n-1)!\prod_{i=1}^{N}\frac{i^{n_i}}{n_i!} \quad . \tag{B2}$$

Here, $n!/\prod n_i!$ is the number of possible unordered distributions of clusters, $\prod i^{n_i}$ corresponds to the choice of an element in each cluster, $(n-1)!$ defines order in the set of clusters (due to periodicity of the lattice, the choice of the first cluster should be made in advance), and N identifies the position of the head of the first cluster on the lattice.

An exception is the case with only one cluster of size N where there are only N different objects, not N^2 as suggested by the formula (B2), because this cluster has no head. However, the formula (B1) is valid also in this case.

For any ordered sequence of n nonintersecting connected clusters $K_1,\dots,K_n$ of sizes $i_1,\dots,i_n$ covering the lattice, with a distinguished element $m_j \in K_j$, the set of all states with an ordered sequence of n breaks of sizes $i_1,\dots,i_n$ starting with elements $m_1,\cdots,m_n$ is defined by

$$1 > \sigma_{m_1} + p_1(m_1) > \sigma_{m_2}$$

$$+p_2(m_2) > \cdots > \sigma_{m_n} + p_n(m_n) \geq 1 - S \quad , \tag{B3}$$

$$\sigma_{m_j} + p_j(m_j) + p > \sigma_k + p_j(k) + p$$

$$\geq \sigma_{m_j} + p_j(m_j) \quad \text{for } k \in K_j,\ k \neq m_j \quad . \tag{B4}$$

Here, $p_j(k) = \sum_{i \in K_1 \cup \cdots \cup K_{j-1}} p_{i,k}$ is the stress increment at a site $k \in K_j$ due to the breaks in the first $j-1$ clusters. The volume of this set is $S^n p^{N-n}/n!$.

Once again, an exception appears in the case of one cluster of size N where the last broken element receives stress $2p$ in fast time. In this case, in addition to the set

$$1 > \sigma_{m_1} \geq 1 - S;\ \sigma_{m_1} + p > \sigma_k + p \geq \sigma_{m_1}$$

$$\text{for } k \neq m_1 \quad , \tag{B5}$$

the following $N-1$ sets appear for $j \neq m_1$:

$$1 > \sigma_{m_1} \geq 1 - S,\ \sigma_{m_1} + p > \sigma_j + 2p \geq \sigma_{m_1},$$

$$\sigma_{m_1} + p \geq \sigma_k + p \geq \sigma_{m_1} \tag{B6}$$

for $k \neq m_1, j$. The total volume of sets (B5) and (B6) is equal to NSp^{N-1}. This, in combination with (B2), proves (B1).

Theorem 1. (a) The volume of all periodic trajectories with n clusters is equal to

$$V(n,N) = \frac{N}{n}\binom{N+n-1}{2n-1} S^n p^{N-n} \quad . \tag{B7}$$

(b) Let $V(N) = \sum_n V(n,N)$ be the total volume of all periodic trajectories. Then

$$\sum_{N=1}^{\infty} V(N) z^N = \frac{Sz(1+pz)}{(1-pz)(1-z+p^2z^2)} \tag{B8}$$

and

$$V(N) \propto \left(\frac{1+\sqrt{1-4p^2}}{2}\right)^N \quad \text{as } N \to \infty \quad . \tag{B9}$$

Theorem 2. Let

$$A_j(N) = \frac{1}{V(N)} \sum_{n_1+2n_2+\cdots+Nn_N=N} n_j V_{n_1,\dots,n_N} \tag{B10}$$

be the mean value of the number of clusters of size j for a randomly chosen periodic trajectory. Then

$$A_j(N) = \frac{jN}{V(N)} \sum_{n=1}^{N} \binom{N+n-j-2}{2n-3} S^n p^{N-n} \quad , \tag{B11}$$

$$\sum_{N=j}^{\infty} A_j(N) \frac{V(N)}{N} z^N = \frac{jSp^{j-1}(1-pz)^2 z^j}{1-z+p^2z^2} \quad , \tag{B12}$$

and

$$A_j(N) \propto jNS\sqrt{\frac{1-2p}{1+2p}} \left(\frac{2p}{1+\sqrt{1-4p^2}} \right)^{j-1} \tag{B13}$$

for $N \gg j$.

Lemma. (See Zelevinsky [23]).

$$\sum_{n_1,\ldots,n_N} \prod_{i=1}^{N} \frac{i^{n_i}}{n_i!} = \frac{1}{n!} \binom{N+n-1}{2n-1} \quad , \tag{B14}$$

where the sum is taken over all integer sequences $(n_1, \ldots, n_N)$ with $n_i \geq 0$ for all i, $n_1 + \cdots + n_N = n$, $n_1 + 2n_2 + \cdots + Nn_N = N$.

Proof. Consider the generating function $g(x,y) \equiv \sum_{n,N=0}^{\infty} \nu(n,N) x^n y^N$, where $\nu(n,N)$ denotes the left side of (B14). We have

$$\begin{aligned} g(x,y) &= \sum_{n_1,\ldots,n_N} \prod_{i=1}^{N} \frac{i^{n_i}}{n_i!} x^{n_i} y^{in_i} = \prod_{i=1}^{\infty} \exp(ixy^i) \\ &= \exp\left(\sum_{i=1}^{\infty} ixy^i \right) = \exp \frac{xy}{(1-y)^2} \\ &= \sum_{n=0}^{\infty} \frac{x^n}{n!} \sum_{i=0}^{\infty} \binom{2n+i-1}{2n-1} y^{n+j} \\ &= \sum_{n=0}^{\infty} \frac{x^n}{n!} \sum_{N=n}^{\infty} \binom{N+n-1}{2n-1} y^N . \end{aligned} \tag{B15}$$

Extracting the coefficient for $x^n y^N$, we have (B14).

Proof of Theorem 1. According to (B1),

$$\begin{aligned} V(n,N) &= \sum_{n_1,\ldots,n_N} V_{n_1,\ldots,n_N} \\ &= N \sum_{n_1,\ldots,n_N} n_j (n-1)! \\ &\quad \times \prod_{i=1}^{N} \frac{i^{n_i}}{n_i!} \times S^n p^{N-n} \quad , \end{aligned} \tag{B16}$$

where the sum is taken over $n_1 + \cdots + n_N = n$, $n_1 + 2n_2 + \cdots + Nn_N = N$. Thus (B7) follows from (B14).

In order to prove (B8) we observe

$$\begin{aligned} -\ln\left(1 - \frac{xy}{(1-y)^2}\right) &= \sum_{n=1}^{\infty} \frac{x^n}{n} \sum_{N=n}^{\infty} \binom{N+n-1}{2n-1} y^N \\ &= \sum_{N=1}^{\infty} \sum_{n=1}^{N} \frac{1}{n} \binom{N+n-1}{2n-1} x^n y^N . \end{aligned} \tag{B17}$$

Taking derivative over y of both sides of (B17) and multiplying by y, we have

$$\frac{xy(1+y)}{(1-y)[(1-y)^2 - xy]} = \sum_{N=1}^{\infty} \sum_{n=1}^{N} \frac{N}{n} \binom{N+n-1}{2n-1} x^n y^N . \tag{B18}$$

Substituting $x = S/p$, $y = pz$ in (B18) we have (B8).

To prove (B9) we represent the right side of (B8) as

$$\frac{Sz(1+pz)}{(1-pz)(1-z+p^2z^2)} = \frac{z_1}{z_1 - z} + \frac{z_2}{z_2 - z} - \frac{2}{1-pz} \quad , \tag{B19}$$

where

$$z_{1,2} = \frac{1 \pm \sqrt{1-4p^2}}{2p^2} \tag{B20}$$

are the roots of $p^2z^2 - z + 1 = 0$. As $z_2 < p^{-1} < z_1$, the second term in this sum defines the asymptotics of coefficients in the power series $\sum V(N) z^N$ for large N, so $V(N) \propto z_2^{-N} = (p^2 z_1)^N$.

Proof of Theorem 2. According to (B1),

$$\begin{aligned} A_j(N) V(N) &= N \sum_{n=1}^{N} \sum_{n_1 + \cdots + n_N = n} n_j (n-1)! \\ &\quad \times \prod_{i=1}^{N} \frac{i^{n_i}}{n_i!} \times S^n p^{N-n} \quad , \end{aligned} \tag{B21}$$

where $n_1 + 2n_2 + \ldots + Nn_N = N$. In order to prove (B11), we have to show that

$$\sum_{n_1 + \cdots + n_N = n} n_j \prod_{i=1}^{N} \frac{i^{n_i}}{n_i!} = \frac{j}{(n-1)!} \binom{N+n-j-2}{2n-3} \quad . \tag{B22}$$

Consider the generating function $g_j(x,y) = \sum_{n,N=0}^{\infty} \nu_j(n,N) x^n y^N$, where $\nu_j(n,N)$ denotes the left side of (B22). We have

$$g_j(x,y) = \sum_{n_1,\ldots,n_N} n_j \prod_{i=1}^{N} \frac{i^{n_i}}{n_i!} x^{n_i} y^{in_i} = jxy^j \prod_{i=1}^{\infty} \exp(ixy^i) = jxy^j \exp\left(\sum_{i=1}^{\infty} ixy^i\right)$$
$$= jxj^j \exp\frac{xy}{(1-y)^2} = \sum_{n=0}^{\infty} \frac{jx^{n+1}}{n!} \sum_{i=0}^{\infty} \binom{2n+i-1}{2n-1} y^{n+i+j}$$
$$= \sum_{n=1}^{\infty} \frac{jx^n}{(n-1)!} \sum_{N=n+j-1}^{\infty} \binom{N+n-j-2}{2n-3} y^N \quad . \tag{B23}$$

Extracting the coefficient for $x^n y^N$, we have (B22)

To prove (B12) we first observe that

$$\frac{1}{1-\frac{xy}{(1-y)^2}} = \sum_{n=0}^{\infty} x^n \sum_{i=0}^{\infty} \binom{2n+i-1}{2n-1} y^{n+i} \quad . \tag{B24}$$

Hence,

$$\frac{jxy^j}{1-\frac{xy}{(1-y)^2}} = j \sum_{n=0}^{\infty} x^{n+1} \sum_{i=0}^{\infty} \binom{2n+i-1}{2n-1} y^{n+i+j}$$
$$= j \sum_{n=1}^{\infty} x^n \sum_{N=n+j-1}^{\infty} \binom{N+n-j-2}{2n-3} y^N . \tag{B25}$$

Substituting $x = S/p$, $y = pz$ in (B25) we have (B12).

To prove (B13) we represent the right side of (B12) as

$$\frac{jSp^{j-1}(1-pz)^2 z^j}{1-z+p^2z^2} = jSp^{j-1}z^j \times \left[1 + \sqrt{\frac{1-2p}{1+2p}}\left(\frac{1}{z_2-z} - \frac{1}{z_1-z}\right)\right], \tag{B26}$$

where z_1 and z_2 are the same as in the proof of Theorem 1. As $z_2 < z_1$, the term with $1/(z_2 - z)$ defines asymptotics of coefficients in the power series in (B26).

APPENDIX C: STRUCTURE OF SIMPLEXES

In case b of the series redistribution model, as well as in the case of parallel redistribution, the analog of proposition 1 is valid for essentially smaller set of states, when only events of size 1 (or degenerate cases when several non-neighboring elements break independently) are allowed. Let $\tau = (i_1, \cdots, i_N)$ be an arbitrary permutation of $(1, \ldots, N)$, $i_j \equiv \tau(j)$. For every i, let $p_i = \sum_{j:\tau(j)<\tau(i)} p_{\tau(i),\tau(j)}$. Then the set of states σ generating periodic trajectories with an ordered sequence $(i_1, \ldots, i_N)$ of single breaks is defined by

$$1 > \sigma_{\tau(1)} + p_1 > \ldots > \sigma_{\tau(N)} + p_N \geq 1 - S \quad . \tag{C1}$$

The volume of this N-dimensional simplex with side S is equal to $S^N/N!$. The union of the sets (C1) over all permutations τ coincides with the set of all periodic trajectories with single breaks. Its volume is S^N.

[1] P. Bak, C. Tang, and K. Wiesenfeld, Phys. Rev. Lett. **59**, 381 (1987); Phys. Rev. A **38**, 364 (1988).

[2] P. Bak and C. Tang, J. Geophys. Res. **94**, 15 635 (1989).

[3] L.P. Kadanoff, S.R. Nagel, L. Wu, and S. Zhou, Phys. Rev. A. **39**, 6524 (1989).

[4] K. Ito and M. Matsusaki, J. Geophys. Res. **95**, 6853 (1990); H. Nakanishi, Phys. Rev. A **41**, 7086 (1990); H. Nakanishi, *ibid.* **43**, 6613 (1991); H. Takayasu and M. Matsuzaki, Phys. Lett. A **131**, 244 (1988); S.R. Brown, C.H. Scholz, and J.B. Rundle, Geophys. Res. Lett. **18**, 215 (1991); H. Takayasu, I. Nishikawa, and H. Tasaki, Phys. Rev. A **37**, 3110 (1988).

[5] H.J.S. Feder and J. Feder, Phys. Rev. Lett. **66**, 2669 (1991).

[6] K. Christensen and Z. Olami, Phys. Rev. A **46**, 1829 (1992).

[7] Z. Olami, H.J.S. Feder, and K. Christensen, Phys. Rev. Lett. **68**, 1244 (1992).

[8] R. Burridge and L. Knopoff, Bull. Seismol. Soc. Am. **57**, 341 (1967).

[9] J. Carlson and J.S. Langer, Phys. Rev. Lett. **62**, 2632 (1989).

[10] J.M. Carlson and J.S. Langer, Phys. Rev. A **40**, 6470 (1989).

[11] J.M. Carlson, Phys. Rev. A **44**, 6226 (1991).

[12] M. Matsuzaki and H. Takayasu, J. Geophys. Res. **96**, 19 925 (1991).

[13] J. Lomnitz-Adler, L. Knopoff, and G. Martinez-Mekler, Phys. Rev. A **45**, 2211 (1992).

[14] A.M. Gabrielov, V.I. Keilis-Borok, T.A. Levshina, and V.A. Shaposhnikov, Comput. Seismology **19**, 168 (1986).

[15] A.M. Gabrielov, T.A. Levshina, and I.M. Rotvain, Phys. Earth Planet. Int. **61**, 18 (1990).

[16] K. Chen, P. Bak, and S.P. Obukhov, Phys. Rev. A **43**, 625 (1991); H.-J. Xu, B. Bergersen, and K. Chen, J. Phys. B **25**, L1251 (1992); B. Barriere and D.L. Turcotte, Geophys. Res. Lett. **18**, 2011 (1991).

[17] A.M. Gabrielov, International Center for Theoretical Physics Report No. H4.SMR/303-36, Trieste, 1988.

[18] A. Diaz-Guilera, Phys. Rev. A **45**, 8551 (1992).

[19] Y.-C. Zhang, Phys. Rev. Lett. **63**, 470 (1989); L. Pietronero, P. Tartaglia, and Y.-C. Zhang, Physica A **173**, 22 (1991).

[20] D. Dhar, Phys. Rev. Lett. **64**, 1613 (1990).

[21] P. Holmes, Phys. Rep. **193**, 137 (1990).

[22] In this case, our models are also equivalent to that introduced by G. Narkounskaia, J. Huang, and D.L. Turcotte, J. Stat. Phys. **67**, 1151 (1992).

[23] A. Zelevinsky (private communication).

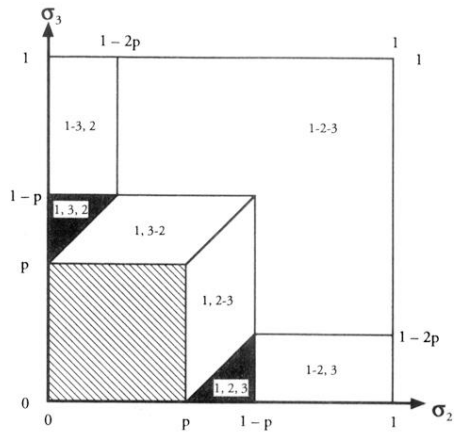

FIG. 1. The Poincaré section $\sigma_1 = 1$ for the three-element configuration, series redistribution model for both cases *a* and *b*. Areas designated by indices correspond to different types of periodic trajectories. Every trajectory starting in the hatched area is unstable and moves into one of the periodic areas. In case *b*, only areas with single breaks, i.e., those designated by $1, 2, 3$ and $1, 3, 2$, (shaded in the figure) are stable.

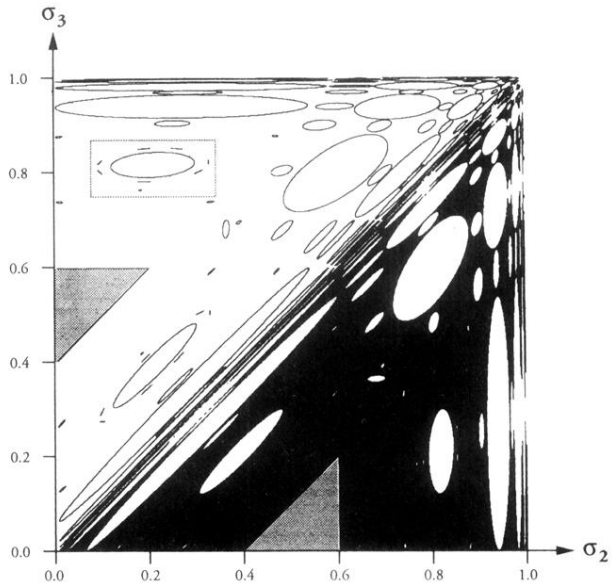

FIG. 2. Poincaré section $\sigma_1 = 1$ for the three-element configuration, parallel redistribution model, $p = 2/5$ or $S = 1/5$. The white triangles correspond to periodic trajectories with single breaks (as in Fig. 1), while the white ellipses correspond to families of invariant tori with quasiperiodic behavior. The figure is symmetric about the diagonal, but the above- and below-diagonal portions highlight different features of the problem. Below the diagonal, the black area defines the chaotic region, while above the diagonal, the boundary between the chaotic and regular behavior is displayed.